Single-File Diffusion in a Box

L. Lizana*
Department of Chemical and Biological Engineering, Chalmers University of Technology, Gothenburg, Sweden
T. Ambjörnsson†
Department of Chemistry, Massachusetts Institute of Technology, Cambridge, Massachusetts 02139, USA
(Received 3 January 2008; published 19 May 2008)

We study diffusion of (fluorescently) tagged hard-core interacting particles of finite size in a finite one-dimensional system. We find an exact analytical expression for the tagged particle probability density function using a Bethe ansatz, from which the mean square displacement is calculated. The analysis shows the existence of three regimes of drastically different behavior for short, intermediate, and large times. The results are in excellent agreement with stochastic simulations (Gillespie algorithm).

DOI: 10.1103/PhysRevLett.100.200601 PACS numbers: 05.40.Fb, 02.50.Ey, 82.39.−k

Introduction.—Recent advances in the manufacturing of nanofluidic devices allow studies of geometrically constrained nanosized particles in quasi-one-dimensional systems in which exclusion effects are important [1]. Situations in which large molecules are hindered to overtake also occur in living systems such as protein diffusion along DNA [2]. Furthermore, biological cells are characterized by a high degree of molecular crowding [3].

In this Letter, with experiments in mind, akin to [4], we focus on diffusive motion of tagged finite-sized hard-core interacting particles (unable to overtake) (Fig. 1). Such single-file systems show interesting behavior where the $t^{1/2}$-scaling (t denotes time) of the mean square displacement (MSD) $\mathcal{S}(t) = \langle [y_{\mathcal{T}}(t) - y_{\mathcal{T},0}]^2 \rangle$ in position $y_{\mathcal{T}}(t)$ of the tagged particle $[y_{\mathcal{T},0} \equiv y_{\mathcal{T}}(0)]$, for an infinite system with fixed concentration, is most striking ($\langle . \rangle$ denotes ensemble average). Also, the probability density function (PDF) $\rho(y_{\mathcal{T}}, t|y_{\mathcal{T},0}) \equiv \rho_{\mathcal{T}}$ is Gaussian [5,6]. Even though single-file diffusion has received much attention [7–10], to our knowledge, very few exact results are given for finite-sized particles in finite systems. One exception is [8] where the PDF for N diffusing point particles on a finite interval was obtained. However, asymptotic expressions were only given when the system was made infinite (keeping the concentration finite). Here, we go beyond previous results in the following ways. First, finite-sized particles are considered, and we show that the N-particle PDF can be written as a Bethe ansatz solution. Second, we perform a (nonstandard) large N-analysis of $\rho_{\mathcal{T}}$, keeping the system size *finite*, showing the existence of three dynamical regimes: (*i*) $t \ll \tau_{\text{coll}} = 1/\varrho^2 D$ where τ_{coll} denotes mean collision time, D the diffusion constant, and $\varrho = N/L$ particle concentration where L is the length of the system; (*ii*) $\tau_{\text{coll}} \ll t \ll \tau_{\text{eq}}$ where $\tau_{\text{eq}} = L^2/D$ is the equilibrium time; and (*iii*) $t \gg \tau_{\text{eq}}$. Notably, only (*i*) and (*ii*) are found in infinite systems. Asymptotic expressions for $\rho_{\mathcal{T}}$ are derived in regimes (*i*)–(*iii*) which show good agreement with Gillespie simulations [11].

Statement of the problem.—We study N hard-core interacting particles with linear size Δ diffusing in a one-dimensional box of length L (Fig. 1). The probability of finding the particles at positions $\vec{y} = (y_1, \ldots, y_N)$ at time t, given that they initially were at $\vec{y}_0 = (y_{1,0}, \ldots, y_{N,0})$, is contained in the N-particle conditional PDF $\mathcal{P}(\vec{y}, t|\vec{y}_0)$ which is governed by the diffusion equation

$$\frac{\partial \mathcal{P}(\vec{y}, t|\vec{y}_0)}{\partial t} = D\left(\frac{\partial^2}{\partial y_1^2} + \ldots + \frac{\partial^2}{\partial y_N^2}\right)\mathcal{P}(\vec{y}, t|\vec{y}_0). \quad (1)$$

Neighboring particles j and $j+1$ are unable to overtake

$$D\left(\frac{\partial}{\partial y_{j+1}} - \frac{\partial}{\partial y_j}\right)\mathcal{P}(\vec{y}, t|\vec{y}_0)\Big|_{y_{j+1}-y_j=\Delta} = 0, \quad (2)$$

ensuring that $y_{j+1} - y_j > \Delta \ \ \forall t$ provided that $y_{j,0} < y_{j+1,0} - \Delta$. The boundaries at $\pm L/2$ are reflecting

$$D\frac{\mathcal{P}(\vec{y}, t|\vec{y}_0)}{\partial y_1}\Big|_{y_1=-(L-\Delta)/2} = D\frac{\mathcal{P}(\vec{y}, t|\vec{y}_0)}{\partial y_N}\Big|_{y_N=(L-\Delta)/2} = 0, \quad (3)$$

and the initial PDF is given by

$$\mathcal{P}(\vec{y}, 0|\vec{y}_0) = \delta(y_1 - y_{1,0}) \cdots \delta(y_N - y_{N,0}), \quad (4)$$

where $\delta(z)$ is the Dirac delta function. The tagged particle PDF studied here is given by [12]

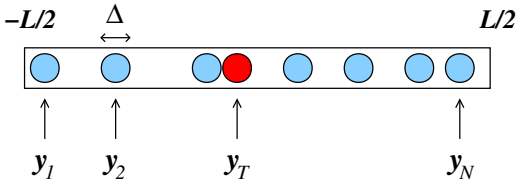

FIG. 1 (color online). Diffusing particles where mutual passage is excluded, i.e., $y_j \le y_{j+1} - \Delta$ for $j = 1, \ldots, N-1$.

$$\rho_{\mathcal{T}} = \frac{1}{\rho_{\mathrm{eq},\mathcal{T}0}} \int_{\mathcal{R}} dy'_1 \cdots dy'_N \int_{\mathcal{R}_0} dy'_{1,0} \cdots dy'_{N,0} \times \delta(y_{\mathcal{T}} - y'_{\mathcal{T}}) \delta(y_{\mathcal{T},0} - y'_{\mathcal{T},0}) \mathcal{P}(\vec{y}', t|\vec{y}'_0) \mathcal{P}_{\mathrm{eq}}(\vec{y}'_0) \tag{5}$$

where $\rho_{\mathrm{eq},\mathcal{T}0} = \int_{\mathcal{R}_0} dy'_{1,0} \cdots dy'_{N,0} \delta(y_{\mathcal{T},0} - y'_{\mathcal{T},0}) \mathcal{P}_{\mathrm{eq}}(\vec{y}'_0)$, with integration regions $\mathcal{R} = \{y_{j+1} - y_j \geq \Delta, j = 1, \ldots, N-1; y_1 \geq -(L-\Delta)/2; y_N \leq (L-\Delta)/2\}$ and $\mathcal{R}_0 = \{y_{j+1,0} - y_{j,0} \geq \Delta, j = 1, \ldots, N-1; y_{1,0} \geq -(L-\Delta)/2; y_{N,0} \leq (L-\Delta)/2\}$. Initially, the particles are distributed according to the equilibrium density,

$$\mathcal{P}_{\mathrm{eq}}(\vec{y}) = \frac{N!}{(L - N\Delta)^N} \Pi_{l=1}^{N-1} \theta(y_{l+1} - y_l - \Delta), \tag{6}$$

i.e., the particles are distributed uniformly in the box. The function $\theta(z)$ is the Heaviside step function.

Bethe ansatz solution.—The Bethe ansatz [9] gives a closed expression for the PDF satisfying Eqs. (1)–(4):

$$\begin{aligned}\mathcal{P}(\vec{x}, t|\vec{x}_0) = \int_{-\infty}^{\infty} \cdots \int_{-\infty}^{\infty} \frac{dk_1 \cdots dk_N}{(2\pi)^N} \\ \times e^{-E(\vec{k})t} \phi(k_1, x_{1,0}) \cdots \phi(k_N, x_{N,0}) \\ \times [e^{i(k_1 x_1 + k_2 x_2 + k_3 x_3 + \ldots + k_N x_N)} \\ + S_{21} e^{i(k_2 x_1 + k_1 x_2 + k_3 x_3 \ldots + k_N x_N)} \\ + S_{21} S_{31} e^{i(k_2 x_1 + k_3 x_2 + k_1 x_3 + \ldots + k_N x_N)} + \ldots],\end{aligned} \tag{7}$$

where $x_1, \ldots, x_N$ and $x_{1,0}, \ldots, x_{N,0}$ are given in terms of $\vec{y}$ and $\vec{y}_0$ according to ($j = 1, \ldots, N$)

$$\ell = L - N\Delta, \qquad x_{j(,0)} = y_{j(,0)} - \Delta\left(j - \frac{N+1}{2}\right), \tag{8}$$

where $-\ell/2 \leq x_1 \leq x_2 \leq \ldots \leq x_N \leq \ell/2$ and $-\ell/2 \leq x_{1,0} \leq \ldots \leq x_{N,0} \leq \ell/2$. The bracket in Eq. (7) contains $N!$ terms corresponding to all permutations of momenta $\vec{k} = k_1, \ldots, k_N$. The quantities S_{lj} are scattering coefficients which contain information about the pair interaction between particles l and j, and are in general functions of k_l and k_j. For the case of a pair interaction on the form given by Eq. (2), $S_{lj} \equiv 1$ ($S_{lj} \equiv 0$ for noninteracting particles) [12]. The time dependence enters through $e^{-E(\vec{k})t}$ with dispersion relation ("energy") $E(\vec{k}) = D(k_1^2 + \ldots + k_N^2)$, obtained from Eq. (1). The functions $\phi(k_j, x_{j,0})$ carry information about the boundary and initial conditions Eqs. (3) and (4), and for the finite box studied here $\phi(k_j, x_{j,0}) = 2\sum_{m=-\infty}^{\infty} \cos[k_j(x_{j,0} + \ell/2)] e^{ik_j(2m+1/2)\ell}$. For an infinite system ($\ell \to \infty$), $\phi(k_j, x_{j,0}) = e^{-ik_j x_{j,0}}$ [9].

Integrating Eq. (7) over $k_1, \ldots, k_N$ gives

$$\begin{aligned}\mathcal{P}(\vec{x}, t|\vec{x}_0) = \psi(x_1, x_{1,0}; t)\psi(x_2, x_{2,0}; t) \cdots \psi(x_N, x_{N,0}; t) \\ + \psi(x_1, x_{2,0}; t)\psi(x_2, x_{1,0}; t) \cdots \psi(x_{N,0}, k_N; t) \\ + \text{remaining permutations of } x_{1,0}, \ldots, x_{N,0},\end{aligned} \tag{9}$$

where $\psi(x_j, x_{l,0}; t) = \int_{-\infty}^{\infty} \frac{dk_j}{2\pi} \phi(k_j, x_{l,0}) e^{ik_j x_j} e^{-Dk_j^2 t}$ is the integral representation of the (free) single particle PDF for particle j. Notably, as $\Delta \to 0$, the N-particle PDF in [8] is recovered. The single particle PDF is also found in [8] (for $\Delta = 0$) but in an unsuitable form for studies of finite systems. We obtained a more convenient expression, where the large time limit is easily tractable, by finding the Laplace transform to $\psi(x_j, x_{l0}; t)$, and inverting it back using residue calculus [12]:

$$\begin{aligned}\psi(x_j, x_{l,0}; t) = \frac{1}{\ell}\Big\{1 + \sum_{m=1}^{\infty} F_m(t)\Big[\nu_m^{(+)} \cos\left(\frac{\pi m x_j}{\ell}\right) \\ \times \cos\left(\frac{\pi m x_{l,0}}{\ell}\right) + \nu_m^{(-)} \sin\left(\frac{\pi m x_j}{\ell}\right) \\ \times \sin\left(\frac{\pi m x_{l,0}}{\ell}\right)\Big]\Big\},\end{aligned} \tag{10}$$

where $\nu_m^{(\pm)} = 1 \pm (-1)^m$ and $F_m(t) = e^{-(m\pi)^2 Dt/\ell^2}$.

Tagged particle density.—Integrating Eq. (9) according to Eq. (5) [8] leads to an exact form of the tagged particle PDF in terms of Jacobi polynomials $P_n^{(\alpha,\beta)}(z)$ [13], given by [14]

$$\begin{aligned}\rho_{\mathcal{T}} = \frac{(N_R + N_L - 1)!}{N_L! N_R!} (\psi_L^L)^{N_L} (\psi_R^R)^{N_R} \\ \times \Big\{(N_L + N_R)\psi\Phi(0,0,0;\xi) + N_L^2 \frac{\psi_L \psi^L}{\psi_L^L} \Phi(1,0,0;\xi) \\ + N_R^2 \frac{\psi_R \psi^R}{\psi_R^R} \Phi(0,1,0;\xi) + N_R N_L \Big[\frac{\psi_R \psi^L}{\psi_R^L} + \frac{\psi_L \psi^R}{\psi_L^R}\Big] \\ \times \Phi(0,0,1;\xi)\Big\},\end{aligned} \tag{11}$$

where $\xi = \xi(y_{\mathcal{T}}, y_{\mathcal{T},0}, t) = \psi_R^L \psi_L^R / (\psi_R^R \psi_L^L)$, $N_L(N_R)$ denotes the number of neighbors to the left (right) of the tagged particle, and

$$\begin{aligned}\Phi(a,b,c;\xi) = \frac{[N_L - (a+c)]!(N_R - b)!}{[N_L + N_R - (a+b+c)]!} \\ \times (1-\xi)^{N_L - (a+c)} \xi^c P_{N_L - (a+c)}^{(c, N_R - N_L + a - b)}\left(\frac{1+\xi}{1-\xi}\right).\end{aligned} \tag{12}$$

Arguments $y_{\mathcal{T}}$, $y_{\mathcal{T},0}$, and t were left implicit. Also,

$$\psi_L^L = \frac{1}{2} + \frac{x_{\mathcal{T}}}{\ell} + \left(\frac{1}{2} + \frac{x_{\mathcal{T},0}}{\ell}\right)^{-1} \sum_{m=1}^{\infty} K_m F_m(t)$$
$$\psi_R^R = \frac{1}{2} - \frac{x_{\mathcal{T}}}{\ell} + \left(\frac{1}{2} - \frac{x_{\mathcal{T},0}}{\ell}\right)^{-1} \sum_{m=1}^{\infty} K_m F_m(t)$$
$$\psi^L = \frac{1}{2} + \frac{x_{\mathcal{T}}}{\ell} + \sum_{m=1}^{\infty} J_m(x_{\mathcal{T}}, x_{\mathcal{T},0}) F_m(t)$$
$$\psi_L = \frac{1}{\ell} + \frac{1}{\ell}\left(\frac{1}{2} + \frac{x_{\mathcal{T},0}}{\ell}\right)^{-1} \sum_{m=1}^{\infty} J_m(x_{\mathcal{T},0}, x_{\mathcal{T}}) F_m(t) \quad (13)$$
$$\psi_R = \frac{1}{\ell} - \frac{1}{\ell}\left(\frac{1}{2} - \frac{x_{\mathcal{T},0}}{\ell}\right)^{-1} \sum_{m=1}^{\infty} J_m(x_{\mathcal{T},0}, x_{\mathcal{T}}) F_m(t),$$

where

$$K_m = \frac{1}{(m\pi)^2}\left[\nu_m^{(+)} \sin\left(\frac{m\pi x_{\mathcal{T}}}{\ell}\right)\sin\left(\frac{m\pi x_{\mathcal{T},0}}{\ell}\right) + \nu_m^{(-)} \cos\left(\frac{m\pi x_{\mathcal{T}}}{\ell}\right)\cos\left(\frac{m\pi x_{\mathcal{T},0}}{\ell}\right)\right]$$
$$J_m(z, z') = \frac{1}{m\pi}\left[\nu_m^{(+)} \sin\left(\frac{m\pi z}{\ell}\right)\cos\left(\frac{m\pi z'}{\ell}\right) - \nu_m^{(-)} \cos\left(\frac{m\pi z}{\ell}\right)\sin\left(\frac{m\pi z'}{\ell}\right)\right]. \quad (14)$$

Normalization gives $\psi^R = 1 - \psi^L$, $\psi_L^R = 1 - \psi_L^L$, and $\psi_R^L = 1 - \psi_R^R$, which completely determines $\rho_{\mathcal{T}}$. A MATLAB implementation of $\rho_{\mathcal{T}}$ is available upon request.

Figures 2 and 3 illustrate the typical behavior of the finite single-file system via stochastic simulations and $\rho_{\mathcal{T}}$. Figure 2 shows particle trajectories produced by the Gillespie algorithm (a Monte Carlo-like algorithm based on a lattice model which is equivalent to the master equation [11]). Figure 3(a) illustrates the time evolution of $\rho_{\mathcal{T}}$ for one tagged particle in the middle of the ensemble, and one by the edge at short (solid line), intermediate (dashed line), and large times (dotted line). The agreement between the analytical result Eq. (11) and the stochastic simulation is excellent. Examples of the equilibrium PDF compared to the point-particle case $\Delta = 0$ is shown in panel (b).

Three dynamical regimes.—Figure 4 shows the results of a numerical calculation of the MSD of a tagged particle located in the middle of the system. The solid curves (blue online) were obtained from numerical integration of $\mathcal{S}(t) = \int_{-L/2+\Delta(N_L+1/2)}^{L/2-\Delta(N_R+1/2)} dy_{\mathcal{T}} (y_{\mathcal{T}} - y_{\mathcal{T},0})^2 \rho_{\mathcal{T}}$, using Eq. (11), for $N = \{3, 21, 141\}$. From Fig. 4, three distinct regimes (*i*)–(*iii*) can be distinguished, which become more pronounced as N increases.

In order to attain a deeper understanding of how regimes (*i*)–(*iii*) emerge, ρ_T [Eq. (11)] was analyzed for large N, keeping L finite. A saddle-point approximation of $\Phi(a, b, c; \xi)$ [Eq. (12)] proved unsuitable since it does not hold for all $\xi \in [0, 1]$ (i.e., all times). However, using asymptotic forms of the Jacobi polynomial from [15], a large N-expansion of $\Phi(a, b, c; \xi)$ valid for all ξ could be obtained [16], and asymptotic expressions for ρ_T in (*i*)–(*iii*) and crossover times (τ_{coll} and τ_{eq}) were deduced:

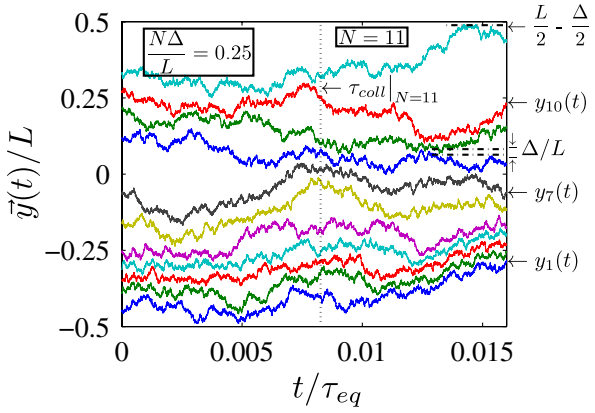

FIG. 2 (color online). Particle trajectories, generated by the Gillespie algorithm, in a system where $N = 11$.

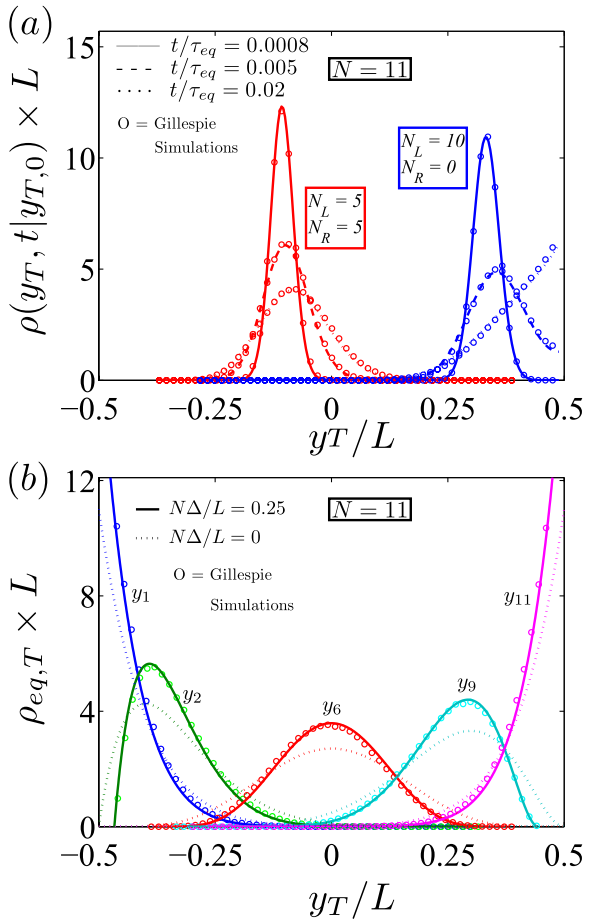

FIG. 3 (color online). (*a*) Tagged PDF [Eq. (11)] for the middle (red online) and the rightmost (blue online) particle, where $N\Delta/L = 0.25$, at three instances of time, with $y_{5,0}/L = -0.15$ and $y_{11,0}/L = 0.3$. (*b*) Equilibrium density [Eq. (16)] compared to the point-particles case and stochastic simulations (∘) ($t/\tau_{\text{eq}} = 2$, 500 lattice points and 10^5 ensembles).

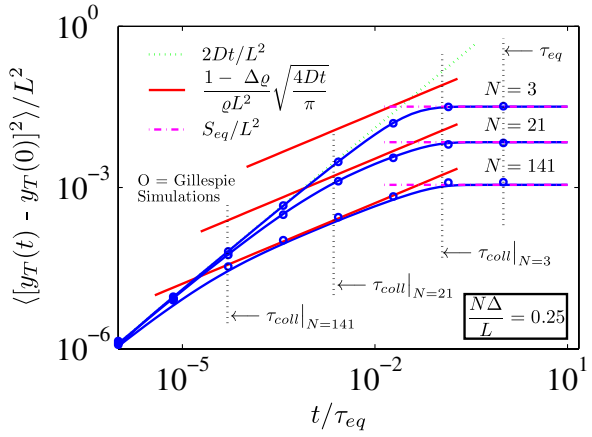

FIG. 4 (color online). Mean square displacement for a tagged particle placed in the middle of the system where $N = \{3, 21, 141\}$. Solid curves (blue online) show numerical calculations of $\mathcal{S}(t)$ based on Eq. (11). Straight lines are approximated analytic results for regimes (*i*)–(*iii*), see text.

(*i*) Short times ($t \ll \tau_{\text{coll}}$): For short times, very few particle (wall) collisions have yet occurred and the particles are (to a good approximation) diffusing independently of each other. In this limit, ρ_T is Gaussian $\rho_{\mathcal{T}} = (4\pi Dt)^{-1/2}\exp[-(y_{\mathcal{T}} - y_{\mathcal{T},0})^2/(4Dt)]$, with MSD $\mathcal{S}(t) = 2Dt$, which is in agreement with the numerical integration of Eq. (11), see Fig. 4.

(*ii*) Intermediate times ($\tau_{\text{coll}} \ll t \ll \tau_{\text{eq}}$): Here, the dynamics is dominated by particle collisions, leading to single-file behavior: $\mathcal{S}(t) \propto t^{1/2}$ (Fig. 4). The PDF in this regime (for particles located not too close to the edges) is

$$\rho_{\mathcal{T}} = \frac{1}{\sqrt{2\pi}}\left(\frac{1}{\frac{4Dt}{\pi}(\frac{1-\varrho\Delta}{\varrho})^2}\right)^{1/4}\exp\left(-\frac{(y_{\mathcal{T}} - y_{\mathcal{T}0})^2}{2\sqrt{\frac{4Dt}{\pi}(\frac{1-\varrho\Delta}{\varrho})^2}}\right) \quad (15)$$

which is a Gaussian with a concentration dependent MSD $\mathcal{S}(t) = [(1-\varrho\Delta)/\varrho]\sqrt{4Dt/\pi}$. Thus, the simple rescaling $\varrho \to \varrho/(1-\varrho\Delta)$ takes us from previous point-particle results [5,6] to the finite particle case.

(*iii*) Large times ($t \gg \tau_{\text{eq}}$): For large times, $\rho_{\mathcal{T}}$ reaches equilibrium and $\mathcal{S}(t)$ is constant (Fig. 4). The equilibrium density $\rho_{\text{eq},\mathcal{T}}$ is found using $\lim_{t\to\infty}\xi = 1$, leading to $\lim_{\xi\to 1}\Phi = 1$ [17], and a large t expansion of Eq. (13):

$$\rho_{\text{eq},\mathcal{T}} = \frac{1}{(L-N\Delta)^N}\frac{(N_L + N_R + 1)!}{N_L!N_R!} \times\left(\frac{L}{2} + y_{\mathcal{T}} - \Delta(1/2 + N_L)\right)^{N_L} \times\left(\frac{L}{2} - y_{\mathcal{T}} - \Delta(1/2 + N_R)\right)^{N_R}. \quad (16)$$

Notably, Eq. (16) can also be found by direct integration of Eq. (6), or from entropy arguments [12]. The MSD $\mathcal{S}(t\to\infty) \equiv \mathcal{S}_{\text{eq}}$ when $N_L = N_R$ is

$$\mathcal{S}_{\text{eq}} = \left(\frac{1}{4}\right)^{N_R+1}\left(\frac{L-N\Delta}{2}\right)^2\frac{\Gamma(1/2)\Gamma(2(N_R+1))}{\Gamma(N_R+1)\Gamma(N_R+5/2)}, \quad (17)$$

where $\Gamma(z)$ is the gamma function.

Conclusions.—We have found an exact solution to a nonequilibrium many-body statistical mechanics problem involving finite-sized particles diffusing in a finite system. The analysis showed the existences of three different regimes for which exact analytical expressions of the tagged particle PDF were found. The results showed excellent agreement with simulations. Tagged particle motion showed sensitivity to environmental conditions (e.g., concentration and system size), suggesting that fluorescently labeled nanoparticles could be used as tiny sensors.

We thank Owe Orwar, Bob Silbey, Mehran Kardar, Ophir Flomenbom, and Michael Lomholt for valuable discussions and comments. T. A. acknowledges the support from the Knut and Alice Wallenberg Foundation.

*lizana@fy.chalmers.se
†ambjorn@mit.edu

[1] C. Dekker, Nature Nanotechnology **2**, 209 (2007).
[2] M. A Lomholt, T. Ambjörnsson, and R. Metzler, Phys. Rev. Lett. **95**, 260603 (2005).
[3] R. J. Ellis and A. P Milton, Nature (London) **425**, 27 (2003).
[4] B. Lin, M. Meron, B. Cui, S. A. Rice, and H. Diamant, Phys. Rev. Lett. **94**, 216001 (2005).
[5] M. Kollmann, Phys. Rev. Lett. **90**, 180602 (2003).
[6] T. E. Harris, J. Appl. Probab. **2** 323, (1965).
[7] D. G. Levitt, Phys. Rev. A **8**, 3050 (1973); K. W. Kehr, R. Kutner, and K. Binder, Phys. Rev. B **23**, 4931 (1981).
[8] C. Rödenbeck, J. Kärger, and K. Hahn, Phys. Rev. E **57**, 4382 (1998).
[9] G. M. Schütz, J. Stat. Phys. **88**, 427 (1997).
[10] Q. H. Wei, C. Bechinger, and P. Leiderer, Science **287**, 625 (2000).
[11] D. Gillespie, J. Comput. Phys. **22**, 403 (1976).
[12] T. Ambjörnsson and L. Lizana, (to be published).
[13] M. Abramowitz and I. A. Stegun, *Handbook of Mathematical Functions* (Dover, New York, 1964).
[14] For $\Delta = 0$, Eq. (11) is related to Eq. (61) in [8] through recursion relations of the Jacobi Polynomial, found in, e.g., [13].
[15] D. Elliott, Math. Comput. **25**, 309 (1971).
[16] $\Phi(a,b,c;\xi)|_{N\gg 1} \approx (N_R - b)!(N_L - a)!/[N - 1 - (a + b + c)]!\{2/[N - (a + b + c)]\}^c\xi^{c/2-1/4}(1-\xi)^{[N-(a+b+c)]/2}\times\zeta^{1/2}I_c\{[N - (a + b + c)]\zeta\}[1 - \mathcal{O}(N^{-1})]$, where $I_c(z)$ is the modified Bessel function of the second kind and $\zeta = \log[(1 + \sqrt{\xi})/(1 - \sqrt{\xi})]/2$. The regimes are given by $(N \gg 1)$: (*i*) $N\zeta \ll 1$; (*ii*) $N\zeta \gg 1$, $\zeta \ll 1$; (*iii*) $\zeta \gg 1$ [12].
[17] The function $\Phi(a,b,c;\xi)$ can be expressed in terms of the Gauss hypergeometric function $\Phi(a,b,c;\xi) =_2 F_1[-N_L + a, -N_R + b, -(N_L + N_R) + a + b + c; 1 - \xi]$ for which $\lim_{\xi\to 1}\Phi(a,b,c;\xi) = 1$.